



## Determination of Limiting Deformations at Testing Cylindrical Samples for Tension

I. Iu. Kyrytsya, O. V. Petrov, I. V. Vishtak\*, S. I. Sukhorukov

Vinnitsia National Technical University, Ukraine

\*E-mail: [innavish322@gmail.com](mailto:innavish322@gmail.com)

Received: 27 December 2023; Revised 20 January 2024; Accept 1 February 2024

### Abstract

This paper proposes a method for calculating limiting deformations under conditions of localized deformation during tensile testing. The method for calculating limiting deformations was used to construct plasticity diagrams under conditions of strain localization under uniaxial tension.

The plasticity diagram is one of the material functions that forms the technological map of the material. The plasticity diagram displays the properties of a material depending on the degree of deformation and the stress state scheme.

According to the studies carried out in this work, it was established that the critical increase in plasticity with increasing stress state indicator is explained by the influence of three factors: the strain gradient, the history of deformation and the third invariant of the stress tensor.

The obtained dependencies make it possible to construct plasticity diagrams for materials whose destruction is preceded by localized deformation in the form of a "neck".

This work establishes the quantitative influence of these three factors on the magnitude of the limiting deformations of a sample stretched to the point of failure.

Application plasticity diagrams constructed using the proposed methods for cold plastic deformation processes, depending on the type of deformation path and the features of metal rheology, clarifies the value of the used plasticity resource of the metal, which allows to reduce the number of defective products for processes whose modes are calculated according to limit deformations.

**Keywords:** limiting deformations, stress state indicators, deformations gradient, deformation history, stress tensor, deformation tensor, plasticity diagram, tension testing.

### Introduction

In the theory of pressure processing of metals, where large plastic deformations are considered (limiting deformations) of such standard mechanical characteristics as yield stress –  $\sigma_{0,2}$ , elastic stress –  $\sigma_{el}$ , proportionality stress –  $\sigma_{pr}$ , strength stress –  $\sigma_{st}$ , as well as plasticity characteristics – relative residual elongation –

$\delta = \frac{l_i - l_0}{l_0} \cdot 100\%$ , relative residual narrowing –  $\psi_n = \frac{A_0 - A_n}{A_0} \cdot 100\%$ , is far from sufficient for describing the

mechanics of metal pressure processing processes.

In the modern phenomenological theory of deformability, the properties of materials are considered in the form of various functions, such as the flow curve of the material; plasticity diagram; calibration schedule: hardness – intensity of stresses – intensity of deformations. These functions form the "technological passport of the material".

When constructing diagrams of plasticity of materials, the method of their construction during stretching of the samples forming the neck remains insufficiently researched.

The development of a technique for constructing plasticity diagrams, which takes into account the peculiarities of deformation localization during the study of tensile materials, remains relevant to this day.



During the stretching of cylindrical samples, the deformation is determined by the diameter of the neck at the time of its initiation, which is significantly lower than that determined by the same diameter after the sample breaks. Therefore, tensile studies allow obtaining sufficiently reliable data only in those cases when a developed neck does not form before failure. In this regard, for a more strict definition of the limiting deformations during stretching of samples, the destruction of which is preceded by a loss of resistance to plastic deformation, it is necessary to have experimental data on the development and accumulation of damage and detected moments preceding the spontaneous development of a macrocrack.

When stretching cylindrical samples from materials, the destruction of which is preceded by the loss of resistance to plastic deformation (formation of the neck), a number of problems arise related to a strict definition:

- accumulated deformation intensity up to the moment of failure (limit deformation) –  $e_p$ ;
- the stress state indicator –  $\eta$  – the ratio of the average stress to the stress intensity.

Strict calculation of  $\eta$  and  $e_p$  during stretching of the samples forming the neck will allow to establish the path of deformation of the material particles from the beginning of the loss of stability to the complete destruction of the sample. As is known, the path of deformation (the rate of change of  $\eta$  and  $e_p$ ) affects the maximum strain intensity accumulated before failure.

With the help of the approaches proposed in this work, material models are formed, which are the basis for calculating the stress-strain state and energy parameters of deformation processes in pressure treatment processes.

### Analysis of recent research and publications

In modern fracture criteria, which have been applied in the problems of metal forming by pressure [1-5], experimental data are used in the form of functions – material characteristics, called plasticity diagrams. The plasticity diagram is one of the functions, which allows in the future to form a technological map of the material.

Plasticity diagrams are obtained by testing materials in tension, compression, torsion, or a combination of these types of tests [6-10].

The calculation of the stress state index  $\eta$  and limit deformation  $e_p$  is carried out according to the method obtained on the basis of the solution of the problem of the stress state in the neck, proposed by N.N. Davidenkov and N.I. Spiridonova [11]. This technique was based on the Haar-Karman assumption about the equality of the circular stress to one of the main stresses in the meridional plane. As shown in [12-14], this hypothesis is valid only when determining deforming forces. When estimating the stress-strain state, this hypothesis leads to errors of unknown magnitude.

As follows from the results of the calculations (Fig. 1.), the limiting deformation determined by the diameter of the neck at the point of rupture is overestimated, and for some materials it reaches a value that exceeds even the value  $e_p$  at shear,  $e_p(\eta = 1) \geq e_p(\eta = 0)$ , while according to the second experiments plasticity decreases with increasing  $\eta$ . This is not related to a change in the stress state pattern in the neck. Since triaxial tension occurs in this region, the  $\eta$  index increases, which should lead to a decrease in plasticity.

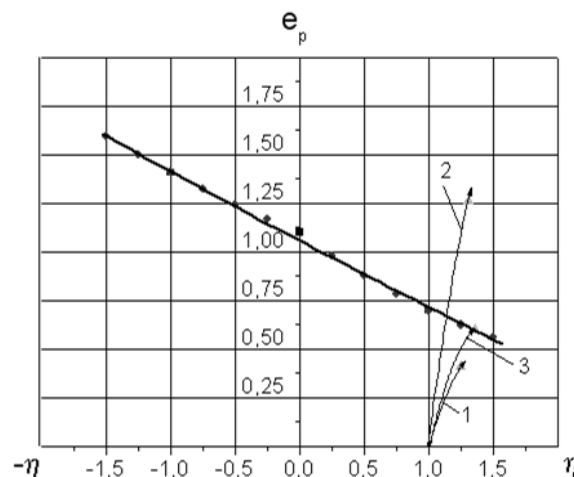


**Fig. 1. Diagram of plasticity of steel 3 and paths of deformation 1,2,3 of material particles: path 1 corresponds to the stretching of the sample before the appearance of critical stable deformation; path 2 – stretching the sample until its complete destruction; path 3 – the appearance of macrocracks before the destruction of the sample.**

In our opinion, this abnormal increase in plasticity can be related to three factors. One of them is the influence of the deformation gradient on plasticity.

In work [10] it is shown that, other things being equal (while the stress state indicator remains unchanged, plasticity increases). It is also shown that if  $grad e_u$  varies from 0 to 0,06, then plasticity increases by  $\Delta e_u = 0,15$ .

There are reasons to assume that the deformation gradient in the neck area can influence the growth of plasticity.

The second factor that can influence the increase in plasticity in the neck region is the rate of change of the stress state indicator, in other words, the history of deformation.

Thus, work [11] shows that when  $\frac{d\eta}{de_u} > 0$ , plasticity increases, and when  $\frac{d\eta}{de_u} < 0$ , plasticity decreases.

The reason for this abnormal increase in plasticity should also be sought in the very nature of the destruction. The highest  $\eta$  is obtained in the center of the neck on the axis of the sample. According to this, the macrocrack originates in this place.

Thus, in the work [12] shows an X-ray picture of the neck of an aluminum round sample immediately before destruction, while a macrocrack is observed in the center of the cross-section, which did not reach the edges of the cross-section contour. Therefore, the calculation of the limit deformation according to the formula

$e_p = 2 \ln \frac{d_0}{d_n}$  is incorrect.

According to the observations made [13], the deformation is determined by the diameter of the neck at the time of its initiation, which is significantly lower than that determined by the same diameter after the sample rupture. Therefore, tensile studies allow obtaining sufficiently reliable data only in those cases when a developed neck does not form before failure. In this regard, for a more strict definition of the limiting deformations during stretching of samples, the destruction of which is preceded by a loss of resistance to plastic deformation, it is necessary to have experimental data on the development and accumulation of damage and detected moments preceding the spontaneous development of a macrocrack.

For further experiments, we chose steel 3, because this metal is ductile due to its low carbon content, and the formation of a neck is clearly visible on the samples during tension.

When testing for tension, compression, torsion or tension together with torsion, it is necessary that the constancy the dimensionless stress state indicators is maintained. Such indicators, which are widely used in the theory of deformability, are:

$$\eta = \frac{I_1(T_\sigma)}{\sqrt{3I_2(D\sigma)}} = \frac{3\sigma}{\sigma_i}, \quad (1)$$

$$\chi = \frac{\sqrt[3]{I_3(T_\sigma)}}{\sqrt{3I_2(D\sigma)}} = \frac{\sqrt[3]{\sigma_1\sigma_2\sigma_3}}{\sigma_i}, \quad (2)$$

where  $I_1(T_\sigma)$ ,  $I_3(T_\sigma)$  are the respectively the first and third invariants of the stress tensor;

$I_2(T_\sigma)$  is the second invariant of the stress deviator;

$\sigma_1, \sigma_2, \sigma_3$  are the principal stresses;

$\sigma$  is the average stress;

$\sigma_i$  is the stress intensity.

Experimentally plotted curves  $e_p(\eta, \chi)$

$$e_p = \int de_{ij} \quad (3)$$

approximate and the resulting functions are called the plasticity diagram [12, 13].

When carrying out experiments, it is necessary to observe the conditions  $\eta = const, \chi = const$ .

However, the specified condition of the constancy of the stress state index during the test is often not performed. The deformation path of the material particles  $\eta(e_i)$ , for example, under tension can vary from  $\eta = 1$  (uniaxial tension) to  $\eta > 2$  (biaxial tension). As shown in work [14], the limiting deformation turns out to be dependent on the history of deformation and in some cases exceeds the value of  $e_p(\eta=0)$  (torsion), which contradicts the physical concepts.

Besides, as shown in work [14], when tensile samples made of materials, the destruction of which is preceded by localization and deformation in the form of a "neck", the value of  $e_p(\eta=1)$  is influenced by the volumetric stress state schema. As an indicator of the stress state in work [14], the indicator (2) is proposed, which takes into account the influence of the third invariant of the stress tensor. In the same work, it was shown that  $I_3(T_\sigma)$  affects the plasticity  $e_p(\eta=1)$ . In the range of the index  $1 \geq \eta \geq -2$ , the diagram is influenced by the third

invariant of the stress tensor. In the region  $I > \eta > 0$ , the third invariant increases plasticity (in comparison with the plasticity diagram plotted under the conditions  $I_3(T_\sigma) = 0$ ) (Fig. 2).

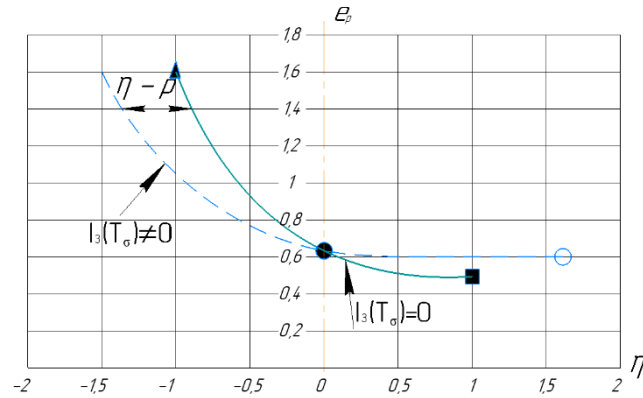


Fig. 2. Diagram of plasticity for steel 20

■ – stretching; ▲ – compression; ● – torsion; ○ –  $\eta=1,55$ ; ---- –  $I_3(T_\sigma) \neq 0$ ; — –  $I_3(T_\sigma) = 0$

In work [14] is stated that at a constant stress state index, the deformations gradient increases plasticity. This work presents the results of experiments carried out on samples of high-speed steels P12 and P18 of square and rectangular cross-section. Different deformation gradients are achieved by different cross-sectional sizes. The samples were deformed under conditions of pure bending up to fracture. Deformations were determined experimentally by the method of dividing grids applied with a Vickers hardness tester with a base of 1 mm on the side surface.

Deformation degree at pure bending

$$e_i = \frac{\sqrt{2}}{3} \sqrt{(e_r - e_\theta)^2 + (e_\theta - e_z)^2 + (e_z - e_r)^2} . \tag{4}$$

Deformation tensor characterizing the deformations gradient

$$T_e = \sqrt{\left(\frac{\partial e_r}{\partial r}\right)^2 + \left(\frac{\partial e_\theta}{\partial r}\right)^2 + \left(\frac{\partial e_z}{\partial r}\right)^2 + 2\left(\frac{e_r}{r_0} - \frac{e_\theta}{r_0}\right)^2} . \tag{5}$$

The derivatives were determined as the tangent of the angle of inclination of the tangents to the corresponding dependences at the points adjacent to the fracture site. The radii of curvature were determined for the stretched surface in the area adjacent to the rupture line.

The stress state index ( $I$ ) equal to the ratio of the first invariant of the stress tensor to the stress intensity was calculated by the formula

$$\eta = 2 \frac{e_r}{e_i} . \tag{6}$$

The value of  $\eta$  practically did not differ from unity.

**Aim of the article** is to develop the method of calculating limiting deformations at constructing plasticity diagrams at conditions of localization deformation under uniaxial tension. To investigate what factors influence the abnormal increasing in plasticity with increasing stress index under uniaxial tension.

**Methods**

In the process of the research the following methods have been used: analysis of the literature sources, mathematical modelling of the processes, using basic laws of solid-state mechanics, theory of modelling and system analysis, numerical methods of studying mathematical models, described by the systems of differential and algebraic equations, computer processing of information.

Methods of mathematics and applied theory of plasticity, phenomenological theory of deformability were also used to solve the problems posed in the work. The hardness method, the experimental-calculation method of

grids and the approximate engineering method for calculating the stress-strain state were also used. The results of the research were processed using the methods of mathematical statistics.

Experimental studies performed using physical modeling methods. The physical and mechanical properties of the studied materials were determined using standard equipment. Specially made devices were also used. Experiments were conducted in laboratory and production conditions.

The problems were solved, using the package of the applied programs MathCAD.

## Results

Based on the processing of the experimental data obtained in work [15], proceeding from the theory of diffusion of dislocations and the assumption that at  $\eta = \text{const}$  the intensity of deformations is proportional to the density of dislocations, the following equation is proposed

$$e_p = b \exp(\beta t) + \frac{4}{3} \frac{\frac{\partial e_i}{\partial x} \int \sqrt{Dt}}{x=l} \sqrt{\pi} \quad (7)$$

Dependence (7) is verified by experiments:  $\beta t = 2,079$ ,  $Dt = 16,78 \text{ mm}^2$ ,  $b = 0,00895$ .

$$e_p = \frac{1}{2} \left( \text{grad } e_i \right)^{0,3} \quad (8)$$

or

$$\text{grad } e_i = \exp \left( \frac{\ln \frac{e_p}{0,5}}{0,3} \right) \quad (9)$$

The results obtained make it possible to take into account the effect of the deformations gradient at constructing the plasticity diagram.

The work [14] investigated the limiting deformation on the contour of the central circular hole in stretched plates 50 mm wide and 2 mm thick made of steel 3. The plates were stretched by a stepwise increasing load. A dividing grid with a base of 0,1 mm is applied on the plates. The specific deformations  $e_i$  were measured.

The obtained results of the dependence of the limiting deformation intensity on the deformations gradient were approximated by the relation

$$e_p = B \left( \text{grad } e_i \frac{1}{\text{mm}} \right)^n \quad (10)$$

or

$$\text{grad } e_i \frac{1}{\text{mm}} = \exp \left( \frac{\ln \frac{e_p}{B}}{n} \right) \quad (11)$$

where  $B = 0,849$ ,  $n = 0,258$ .

The greatest inhomogeneity of the stress-deformation state is also found in this type of test as torsion ( $\eta = 0$ ).

With a constant stress state index ( $\eta = 0$ ), it is possible to carry out experiments on torsion of samples with a diameter  $d = 20, 15, 10, 7,5, 5 \text{ mm}$ .

Along the generatrix of the cylindrical samples with the help of a vernier caliper, a longitudinal risk was drawn. After fracture, the angles of inclination of the helical lines near the fracture site were measured using an instrumental microscope. The degree of deformation was determined by the formula

$$e_p = \frac{\text{tg } \alpha}{\sqrt{3}} \quad (12)$$

The diameter of the sample and the length of the working part were also measured before and after destruction. In the case under consideration, these parameters practically did not change. Consequently, the torsion was constrained, i.e. axial compressive stresses appeared, however, as shown in [13], they are two orders of magnitude less than tangential ones, and the elongation of the samples was practically absent.

Therefore, the hypothesis of flat sections is performed  $e_z(z) = const \cong 0, \sigma_z \cong 0$ .

The quadratic invariant of the deformation tensor  $T_e$  at torsion is

$$T_e = \left[ \left( \frac{e_z \theta}{r} \right)^2 + \left( \frac{\partial e_z \theta}{\partial r} \right)^2 \right] \frac{1}{2}. \quad (13)$$

At torsion  $grad e_i = \frac{de_i}{dr} \cdot \frac{1}{e_{i \max}} = \frac{d\gamma}{dr} \cdot \frac{1}{\gamma_{\max}}$ , that is, with a radius  $r = 4$  mm,

$$grad e_i = \frac{1}{r} = 0,25 \cdot \frac{1}{mm}.$$

Among the many approximations [13, 15] and plasticity diagrams [10, 11], let us dwell on those for which the approximation coefficients have a physical meaning. So in work [11] an approximation of the form is given:

$$e_p(\eta) = e_p(\eta=0) \exp(-\lambda_i \eta). \quad (14)$$

where  $e_p(\eta=0)$  – limiting deformation at shear (torsion);  $\lambda_i$  – respectively:

$$\lambda_1 = \ln \frac{e_p(\eta=0)}{e_p(\eta=1)} \quad (15)$$

is the coefficient of sensitivity of plasticity to a change in the stress state diagram in the region of the index  $1 \geq \eta \geq 0$ ;

$$\lambda_2 = \ln \frac{e_p(\eta=-1)}{e_p(\eta=0)} \quad (16)$$

is the coefficient of sensitivity of plasticity to a change in the stress state diagram in the region of the index  $0 \geq \eta \geq -1$ .

In fig. 3 shows a diagram of plasticity of high-speed steel R18 approximated using formula (14), where  $\lambda_1 = 1,31$ ,  $\lambda_2 = 1,26$ . The specified material was chosen due to the fact that when the samples of this material are stretched, a "neck" is not formed.

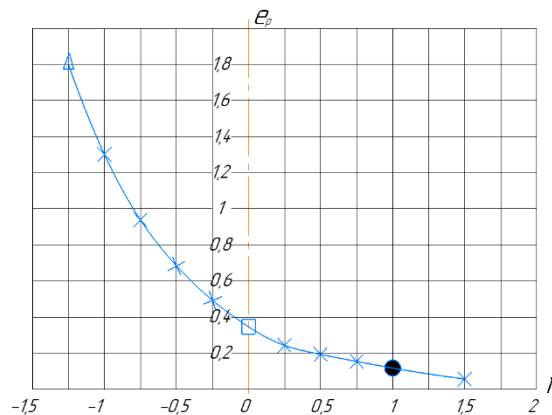


**Fig. 3. Diagram of plasticity of high-speed steel R18**  $\blacktriangle$  –  $e_p(\eta=-1)$ ;  $\blacksquare$  –  $e_p(\eta=0)$ ;  $\bullet$  –  $e_p(\eta=1)$ ;  $\times$  – calculation by the formula (14)

In semilogarithmic coordinates  $\lambda_i$  are the tangents of the slope of the straight lines plotted in the coordinates  $e_p(\eta)$ . The coefficient  $\lambda_i$  ( $i = 1, 2$ ) is essentially the coefficient of plasticity "sensitivity" to changes in the stress state diagram. The greater the value of these coefficients, the more intensive the growth of plasticity occurs with increasing hydrostatic pressure.

A similar idea of the physical essence of the coefficients  $\lambda$  was later published in the work [13], in which, from the point of view of the physics of metals, the expediency of introducing coefficients of "sensitivity" of plasticity to a change in the index  $\eta$  is shown. Thus, in this work, the inflections in the plasticity diagrams plotted in semilogarithmic coordinates are associated with the index of the relaxation capacity (plasticity) of polycrystals  $n$ :

$$n = \frac{d \ln \sigma}{d \ln e} , \quad (17)$$

and the quantities  $e_p$ ,  $\delta$ ,  $\psi$  are a consequence of the quantity  $n$  (but not only of it alone).

Thus, in this work, we have considered the features that arise when constructing plasticity diagrams under conditions of such tests as uniaxial tension and torsion.

Using the example of steel 3, tested under tensile conditions, let us consider our proposed algorithm for constructing plasticity diagrams in the range of variation of the index  $\eta$  from zero to two [14, 15].

Three standard cylindrical samples made of steel 3 (this steel was chosen due to the fact that the destruction of this steel is preceded by localization in the form of a neck) were stretched to various degrees of deformation ( $\delta = \frac{l_i - l_0}{l_0} \cdot 100\%$ ,  $\delta_1 = 2,56\%$ ,  $\delta_2 = 15,92\%$ ,  $\delta_3 = 20,92\%$ ). After deformation (the third sample was destroyed), the geometric parameters were measured (see Table 1).

Table 1

**Geometric parameters and some characteristics of steel samples steel 3**

Sample number	I	II	III
$l$ , mm	12	14	16
$h$ , mm	1,59	1,09	0,99
$d_n$ , mm	5,09	6,08	7,68
$d_0$ , mm	9,5	9,5	9,5
$d_{st}$ , mm	8,01	8,06	8,47
$l_0$ , mm	9,89	9,89	9,89
$\delta$ , %	20,89		
$R$ , mm	11,6	22,79	34,1
$r$ , mm	1,289	1,189	1,164
$e_p$	1,29	0,901	0,442
$d_{cr} = \frac{d_n + d_{st}}{2,22}$ , mm	5,89	6,349	7,268
$e_p^*$	0,915	0,83	0,557

According to work [14], the neck radius was determined by the formula

$$R = \frac{l^2 + 4h^2}{8h} . \quad (18)$$

The stress state index is calculated according to Bridgman, taking into account the approach proposed in works [14, 15]

$$\eta = 1 + 3 \ln \left( 1 + \frac{d_{cr}}{4} \cdot \frac{1}{R} \right) . \quad (19)$$

The work [10] shows a snapshot of the neck of an aluminum sample immediately before destruction. In this case, a macrocrack is observed in the center of the section, which did not reach the edges of the section contour. Therefore, the calculation of the limiting deformation using formula

$$e_p = 2 \ln \frac{d_0}{d_n} \quad (20)$$

significantly overestimates the plasticity.

In works [14, 15], it is proposed to calculate the limiting deformation  $e_p$  by the formula

$$e_p^* = 2 \ln \frac{d_0 \cdot 2,22}{d_n + d_{st}}, \quad (21)$$

where  $d_{st}$  is the cross-sectional diameter of a cylindrical sample at a distance from the minimum neck radius.

Calculation by formula (21) underestimates the plasticity, which corresponds to the physical concepts of the decrease in plasticity with an increase in the index  $\eta$ .

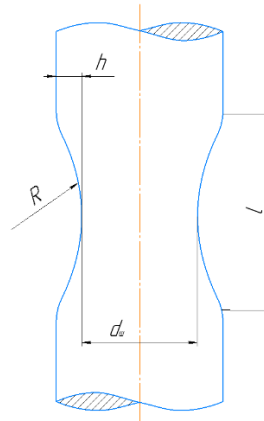


Fig. 4. Scheme of the meridional section of the sample at the site of necking

We will substantiate the possibility of such a calculation based on the above approach on the influence of three factors on plasticity – the deformation gradient, the history of deformation, and the third invariant of the stress tensor.

In the considered example of tension of cylindrical samples of steel 3 in the area of localization of deformation (in the neck), the gradient of deformations overestimates the plasticity by  $\Delta e_i \approx 0,12$ , the history of deformation by an amount  $\theta = \ln \frac{e_p(\eta)}{e_p(\eta = const)} = 0,12 \dots 0,14$ , the third invariant  $I_3(T_\sigma)$  overestimates the plasticity

by 10 – 12%. The calculation of the actual limiting deformation gives the result

$$e_p^a = e_p [1 - (0,12 + 0,13 + 0,12)] = 1,29 [1 - 0,37] = 0,81. \quad (22)$$

Calculation by formula (21) gives satisfactory convergence with calculation by (22)  $e_p^* = 0,915$ .

Using of the plasticity diagram in the form of the dependence of the limiting deformation on the stress state parameter in the known deformation criteria for cold plastic deformation processes can significantly clarify the calculation of the used plasticity resource. In turn, this makes it possible to reduce the probability of fracture (from 30 to 40 %) in the processes of cold plastic deformation, the parameters of which are calculated with minimal margins for fracture deformations, and to expand the technological capabilities of metal pressure processing processes.

## Conclusions

The method of calculating limiting deformations at constructing plasticity diagrams at conditions of localization deformation under uniaxial tension is developed in this work.

The abnormal increase of plasticity with an increase in the stress state index is explained by the influence of three factors: the gradient of deformations, the history of deformation and the third invariant of the stress tensor.

A method of constructing plasticity diagrams has been developed, which takes into account the peculiarities of deformation localization during tensile testing of materials. The method is based on the analysis of the stress-strain state in the neck of the stretched sample in the area of localization of deformation without the inclusion of the Haar-Karman hypothesis and allows determining the limit deformations during stretching of plastic materials.

Using the example of plotting the plasticity diagram of steel 3, the quantitative influence of these three factors on the value of the limiting deformation in the neck of a sample stretched to failure is shown. The total value of the overestimation of the limiting deformation is from 34 to 38 percent.

With the help of the proposed approaches, material models (technological map of the material or passport of the material) are formed, which are the basis for calculating the stress-strain state during the manufacture of blanks (parts), as well as calculating energy parameters of deformation processes.

In this work, modern phenomenological approaches are considered, which will allow structural engineers and technological engineers to create safe structures, structural elements, details, etc., even at the design stage.

The obtained dependencies will allow in the future to provide recommendations for the construction of technological processes for the manufacture of parts or structural elements, etc.

## References

1. Park N., Stoughton T.B., Yoon J.W. (2019). A new approach for advanced plasticity and fracture modelling. IOP Conf. Series: Materials Science and Engineering 651. doi:10.1088/1757-99X/651/1/012097.
2. Gharehbaghi S. Gandomi M., Plevris V., Gandomi A.H., Abdulameer Kadhim A., Mohammed Kadhim H., Ham S.W., Cho J.U., Cheon S.S., Paresi P.R. (2020). Fracture Prediction in Plastic Deformation Processes. *Ductile Fract. Met. Form*, 7, 1–17.
3. Versaillot P.D., Wu Y.F., Zhao Z.L. (2021). An Investigation into the Phenomenon of Macroscopic Plastic Deformation Localization in Metals. *Phys. Conf. Ser.*, 1777, 012067.
4. Paul S.K., Roy S., Sivaprasad S., Bar H.N., Tarafder S. J. (2018). Identification of Post-Necking Tensile Stress–Strain Behavior of Steel Sheet: An Experimental Investigation Using Digital Image Correlation Technique. *Mater. Eng. Perform.*, 27, 5736–5743.
5. Jain A., Mishra A., Tiwari V., Singh G., Singh R.P., Singh S. (2022). Deformation Measurement of a SS304 Stainless Steel Sheet Using Digital Image Correlation Method. *Photonics*, 9, 912. <https://doi.org/10.3390/photonics9120912>.
6. Schwab R., Harter A. (2021). Extracting True Stresses and Strains from Nominal Stresses and Strains in Tensile Testing, 2021, 57, e12396.
7. Achineethongkham K., Uthaisangsk V. (2020). Analysis of forming limit behaviour of high strength steels under non-linear strain paths using a micromechanics damage modelling. *Int. J. Mech. Sci.*, 183, MS105828.
8. Matsuno T., Hojo T., Watanabe I., Shiro A., Shobu T., Kajiwara K. (2021). Tensile deformation behavior of TRIP-aided bainitic ferrite steel in the post-necking strain region. *Technol. Adv. Mater. Methods*, 1, 56–74.
9. Tu S., Ren X., He J., Zhang Z. (2020). Stress–strain curves of metallic materials and post-necking strain hardening characterization. *Fatigue Fract. Eng. Mater. Struct.*, 3–19. <https://doi.org/10.1111/ffe.13134>.
10. Matsuno T., Shoji H., Ohata M. (2018). Fracture-strain measurement of steel sheets under high hydrostatic pressure. *Procedia Manuf.*, 15, 869–876.
11. Ogorodnikov V. A., Dereven'ko I. A., Poberezhnyj M.I. (2011). Karty materialov v processah obrabotki metallov davleniem. [Material Maps for Metal Forming Processes]. *Visnik Nacional'nogo tekhnichnogo universitetu Ukraïni "KPI". Seriya: «Mashinostroenie»*, 52, 62-67.
12. Del' G.D. (1978). *Tekhnologicheskaya mekhanika*. [Technological mechanics]. *Mashinostroenie*, 174.
13. Brünig M., Gerke S., Schmidt M. (2016). Biaxial experiments and phenomenological modeling of stress-state-dependent ductile damage and fracture. *International Journal of Fracture*. Vol. 200, Issue 1-2, 63-76. doi: [10.1007/s10704-016-0080-3](https://doi.org/10.1007/s10704-016-0080-3)
14. Kyrtsya I.Iu. (2014). Osoblyvosti rozrakhunku parametriv napruzhenno-deformovanoho stanu ta pobudovy diahram plastychnosti v zoni lokalizatsii deformatsii pid chas roztyahu tsylindrychnykh zrazkiv. [Peculiarities of calculating the parameters of the stress-strain state and constructing plasticity diagrams in the deformation zone during stretching of cylindrical samples]. *Visnyk Vinnytskoho politekhnichnogo instytutu*, № 2, 101 – 107.
15. Ohorodnykov V. A., Kyrtsya I.Iu., Perlov V.Ie. (2015). *Mekhanika protsesiv kholodnoho plastychnoho deformuvannia visesymetrychnykh zahotovok z hlukhym otvorom* [Mechanics of processes of cold plastic deformation of hexagonal blanks with a blind hole]. Monograph, Vinnytsia: VNTU, 164.

**Кириця І. Ю., Петров О. В., Віштак І. В., Сухоруков С. І.** Визначення граничних деформацій при випробуванні циліндричних зразків на розтяг

Стаття присвячена розрахунку граничних деформацій в умовах локалізованої деформації при випробуванні на розтяг. За допомогою методу розрахунку граничних деформацій побудовано діаграми пластичності в умовах локалізації деформацій при одновісному розтягу.

Діаграма пластичності є однією з функцій матеріалу, яка формує технологічну карту матеріалу та відображає властивості матеріалу в залежності від ступеня деформації і схеми напруженого стану.

Встановлено, що критичне підвищення пластичності зі збільшенням показника напруженого стану пояснюється впливом трьох факторів: градієнта деформації, історії деформації та третього інваріанта тензора напружень. Отримані залежності дають змогу побудувати діаграми пластичності матеріалів, руйнуванню яких передують локалізована деформація у вигляді «шийки».

У роботі встановлено кількісний вплив цих трьох факторів на величину граничних деформацій розтягнутого до руйнування зразка. Прикладні діаграми пластичності, побудовані за запропонованими методами, для процесів холодної пластичної деформації залежно від виду шляху деформації та особливостей реології металу уточнюють величину використаного ресурсу пластичності металу, що дозволяє зменшити кількість бракованих виробів на процеси, режимами яких розраховуються за граничними деформаціями.

**Ключові слова:** граничні деформації, показники напруженого стану, градієнт деформацій, історія деформації, тензор напружень, тензор деформації, діаграма пластичності, випробування на розтяг.